REVISTA MATÉRIA V.27 N.03
ISSN 1517-7076 article e20220033, 2022

Study of simultaneous adsorption efficiency of metals using modified organic and synthetic adsorbents

Emerson Leandro-Silva[1], Angelo Ricardo Favaro Pipi[2], Aroldo Geraldo Magdalena[3], Marina Piacenti-Silva[3]

[1]Universidade Estadual Paulista, Pós-graduação em Engenharia Civil e Ambiental. Avenida Engenheiro Luiz Edmundo Carrijo Coube, 14-01, 17033-360, Bauru, SP, Brasil.

[2]School of Chemical Sciences, National Center for Sensor Research. Dublin City University, Dublin 9, Ireland.

[3]Universidade Estadual Paulista, Faculdade de Ciências, Departamento de Química. Avenida Engenheiro Luiz Edmundo Carrijo Coube, 2085, 17033-360, Bauru, SP, Brasil.

e-mail: emerson.silva@unesp.br, angelfav@gmail.com, aroldo.magdalena@unesp.br, marina.piacenti@unesp.br

ABSTRACT

Water contamination by heavy metals represents a high risk of environmental pollution and a precursor of several human diseases. The presence of these metals at high levels in wastewater treatment plants and industrial effluents motivated the search for remediating these pollutants. Among remediation methods, adsorption is extensively used to decontaminate waters containing these metals. Thus, this study prepared, characterized, optimized, and applied two types of adsorbents to a prepared metal ion solution (PMS): a bioadsorbent based on banana peel flour (BPF) and a synthetic adsorbent based on magnetite encapsulated by chitosan (MEC). A systematic study was performed with PMS containing Al (III), Ba (II), Pb (II), Cu (II), Cr (III), Fe (II), Mn (II), and Zn (II) to determine the best conditions for simultaneous metal ion adsorption Adsorption studies evaluated the experimental adsorption isotherms according to the variation in pH values, the mass of adsorbents, and contact time, and the kinetic study applied pseudo-first- and pseudo-second-order models. The best parameters were the pH of 6, a mass of adsorbents of 25 mg, and fast saturation time of around 10 minutes. The kinetic model that best fitted the process was the pseudo-second-order for all metals in both adsorbents. The PMS adsorption capacity achieved by MEC was higher than BPF. The removal by MEC was Al=Fe=Pb=Cu=Cr> Zn>Mn>Ba, in the percentages of 100, 100, 100, 100, 100, 98, 88, and 76%, respectively. The BPF showed Pb>Fe>Cr>Cu>Al>Zn>Ba>Mn, in the percentages of 97, 67, 63, 50, 46, 45, 44, and 5%, respectively. The results suggest that the affinity between adsorbents with certain metal ions is due to the characteristics of the adsorbent surface and the number of chemical species available in the solution, which may interfere with the adsorptive process. Above all, the percentage of simultaneous removal of metal ions by both adsorbents was relevant, making them promising for remediating heavy metal ions in sanitary sewage after conventional treatment and industrial effluents containing mixed metal ions.

Keywords: Adsorption; *Musa spp*; Heavy Metal; Magnetite; Chitosan.

1. INTRODUCTION

Water is an essential natural resource for maintaining life in our ecosystem. Hence, consciously using and treating water after its use becomes essential to preserve the environment and human life in both present and future generations. Industrial activities produce a significant amount of effluents with chemical pollutants that are harmful to health and the environment and need to be removed [1]. Among the chemical pollutants in most industrial effluents, heavy metals have been gaining special attention for being recalcitrant pollutants in the environment and causing an enormous environmental imbalance. They are also highly toxic to human health and precursors of various diseases, such as heart and neurodegenerative diseases [2]. In this sense, studies seek efficient and economically viable alternatives for remediating effluents containing heavy metals in their ionized form [3]. The adsorption technique is an effective method for treating and removing metal ions in effluents [4]. Activated carbon has long been the most extensively used adsorbent material for adsorption due to its versatility and effectiveness in the adsorptive process for removing metal ions in effluents [5–6]. However, new studies seek other alternatives that are inexpensive and efficient in removing heavy metals [5]. Among the viable techniques for removing heavy metals,

Corresponding Author: Emerson Leandro-Silva Received on 25/02/2022 Accepted on 06/06/2022

DOI: https://doi.org/10.1590/1517-7076-RMAT-2022-0033

bioadsorbents are interesting because they are natural, abundant, renewable, and inexpensive. Bioadsorption has a particular adsorption feature, using vegetable biomass as an adsorbent material for removing metals in aqueous solutions. The bioadsorption process occurs through electrostatic interactions and/or the formation of bonds between metal ions and functional biomass groups [7]. Therefore, bioadsorbents have been extensively studied as alternative materials for treating several types of effluents composed of heavy metals [8]. Among bioadsorbents, the banana peel stands out because it is a fruit abundantly consumed in Brazil and whose peel is usually discarded [9]. Moreover, the banana peel has numerous organic groups responsible for adsorbing metal ions and consists of several groups such as carbonyls, phenols, carboxyls, and hydroxyls from functional groups such as cellulose, holocellulose, lignin, pectic acid, organic acids, and proteins [4–5,10]. These organic functional groups form bonds with metals through electrostatic interactions and ionic and/or covalent chemicals [11].

Another alternative for removing heavy metal ions is using ferromagnetic nanomaterials, which have stood out as a viable alternative because of their high efficiency in removing heavy metal ions in aqueous solutions and simple synthesis process. Magnetites have a strong magnetic response in the presence of an external magnetic field, an attribute that supports their separation from the aqueous medium due to the intrinsic superparamagnetic property of this material [12–13]. Another important aspect of the iron oxide (Fe_3O_4) nanoparticle is the ability of functionalization by compounds that can adsorb metals such as chitosan, APTMS (3-aminopropyltrimethoxysilane), silica, and humic acid, among others, ensuring the removal of toxic metals in aqueous media [14–15]. Another vital property of the functionalized nanoparticle refers to the large surface area due to its small size, which possibly increases the efficiency in adsorbing ions of different metals in aqueous solutions [16]. Among the compounds, chitosan enhances the adsorptive and selective capacities of magnetite due to the presence of amino and cellulosic functional groups responsible for metal adsorption [16] and improves the colloidal stability of this nano-adsorbent in the environment, which is essential for adsorbing metal ions [17].

Given this scenario, the main objective of this study was to investigate the adsorptive efficiency of the Al (III), Ba (II), Pb (II), Cu (II), Cr (III), Fe (II), Mn (II), and Zn (II) metal ions, simultaneously using banana peel flour as a bioadsorbent and magnetite encapsulated by chitosan as a nano-adsorbent in a prepared metal ion solution. The study also aimed to compare the results of characterizations with the adsorptive capacity of these materials.

2. EXPERIMENT

2.1. Reagents

This study used HCl (37% purity, Synth) for the treatment of banana peel flour (BPF), and $FeCl_2.4H_2O$ (98% purity, Dinâmica), $FeCl_3.6H_2O$ (97% purity, Dinâmica), ammonium hydroxide (NH_4OH) (25% purity, Synth), low molecular weight chitosan (75–85% deacetylated, Sigma Aldrich), sodium hydroxide (NaOH) (97% purity, Merck), acetic acid (97% purity, Merck), and nitric oxide (70% purity, Synth) for nanoparticle synthesis.

2.2. Preparation and synthesis of adsorbents

The banana peel flour (BPF) was prepared and treated according to the methodology applied previously [1]. The Fe_3O_4 magnetite was synthesized according to the reference [18] with modifications. Iron oxide-based nanoparticles were produced with the alkaline co-precipitation method and subsequent encapsulation by chitosan (MEC). To encapsulate the magnetites with chitosan, 1 g of low molecular weight chitosan (Aldrich) was added to 400 mL of a 2% acetic acid solution under vigorous stirring until increasing the viscosity (gelatinous). Still under vigorous stirring, the synthesized magnetites were added. This mixture was left under constant stirring for 1 hour at normal atmospheric conditions and room temperature. The precipitate was decanted with a magnet. Then, 200 mL of the supernatant was removed and 50 mL of NaOH (2 mol) was added dropwise aided by a burette under stirring. The final precipitate was separated with a magnet and washed several times with distilled water. Finally, it was dried at 60°C in a forced-air oven.

2.3. Characterizations of adsorbent materials

The BPF and MEC adsorbents were characterized with the following techniques: Scanning Electron Microscopy (SEM), obtained from the FE-SEM microscope, JEOL 7500 F, 10-kV beam, and 500 to 5000 times magnification; Energy-Dispersive X-ray (EDX-SEM) with 10 kV of excitation energy; Fourier Transform Infrared spectroscopy with attenuated total reflection (FTIR ATR Vertex 70 – Bruker), with a scanning range between 4000 and 400 cm^{-1} (32 scans and 4-cm^{-1} resolution) and a diamond crystal as the support. The SEM, EDX, and FTIR analyses were performed with BPF samples *in natura* and after the chemical treatment, and in the nano-adsorbent used in the magnetite samples before and after encapsulation by chitosan and after the adsorption in both adsorbents.

Table 1: Metal ion concentration limits according to the Brazilian legislation.

Metal ions	Al	Ba	Pb**	Cu	Cr	Fe	Mn	Zn
CONAMA[a]	0.100	0.700	0.010	0.009	0.050	0.300	0.100	0.180
PMS*	0.150	1.050	0.060	0.013	0.075	0.450	0.150	0.270

a – Metal ion concentrations in mg L^{-1}; * Prepared metal ion solutions; ** 500% lead in the PMS.

2.4. Prepared metal solution

The prepared metal solution (PMS) was produced to simulate an effluent containing several metals. Therefore, monoelemental reference standards at a concentration of 100 mg L^{-1} (SpecSol Certificate) were used for preparing a multielemental solution. This solution was prepared with the following metal ions: Copper (Cu), Aluminum (Al), Chrome (Cr), Iron (Fe), Barium (Ba), Lead (Pb), Manganese (Mn), and Zinc (Zn). The metal concentrations prepared were 50% higher than the limits recommended by the Brazilian legislation (357/05 CONAMA) for class II receptor bodies [19–20], because in Brazil, the effluent receiving bodies treated are mostly class II (only Pb with 500% due to the detection limit in the analysis). Table 1 shows the Brazilian legislation limits and PMS metal ion concentrations.

2.5. Adsorption studies

Adsorption studies were performed in batch systems with fixed reaction volumes of 0.025 L. The mass of adsorbents in all batches was 100 mg for BPF and MEC, except for the study of adsorbents mass variation. The contact time was fixed at 60 minutes, except for the study of time variation. The temperature studied was room temperature of 26°C (±2). The system remained under continuous agitation throughout the process, averaging 300 rpm, with BPF on a magnetic stirrer and MEC on a mechanical stirrer. Subsequently, BPF and MEC adsorbents were separated from the supernatant aided by a paper filter and an external magnet, respectively.

To assess the adsorptive capacity of BPF and MEC, adsorptive studies were performed with PMS varying the pH value (2 to 8), the concentration of adsorbents (25, 50, 100, 200, and 400 mg), the contact time (10, 20, 40, and 60 minutes), and the interpretation of adsorption kinetics using pseudo-first-order [21] and pseudo-second-order models [22]. All experiments were performed in triplicate. The removal percentage (%) was determined with Equation (1):

$$(\%) = \frac{c_o - c_e}{c_o} \cdot (100) \tag{1}$$

where C_o and C_e are, respectively, the initial and final metal concentrations in the solution, in mg L^{-1}. The adsorptive capacity at equilibrium (qe) was determined with Equation (2) [23]:

$$q_e = \frac{c_o - c_e}{m} \cdot V \tag{2}$$

where m is the mass of adsorbents (g) and V is the volume of the solution (L).

The pseudo-first-order kinetic study was investigated with Equation (3), which refers to the adsorption rate for this kinetic model [21]:

$$\frac{dq_t}{dt} = K_1(q_e - q_t) \tag{3}$$

where K_1 is the velocity constant (min^{-1}), q is the amount of metal adsorbed per amount of adsorbent (mg g^{-1}) in equilibrium, and qt is the amount of metal adsorbed per amount of adsorbent at time t. Therefore, the non-linear form proposed by the kinetic model can be represented with Equation (4) [21]:

$$q_t = q_e(1 - e^{-k_1 t}) \tag{4}$$

After the linearization of Equation (4), the *Ln (qt)* graph was obtained according to *t* with Equation (5), where the K_1 parameter is the slope of the line [21]:

$$ln\,(q_t) = ln\,(q_e) - K_1 t \tag{5}$$

The adsorption rate of the pseudo-second-order kinetic model can be represented with Equation (6) [22]:

$$\frac{dq_t}{dt} = K_2 (q_e - q_t)^2 \tag{6}$$

where K_2 is the velocity constant (g mg^{-1} min^{-1}). The nonlinear form of the pseudo-second-order kinetic model is represented with Equation (7) [22]:

$$q_t = \frac{q_e^2 K_2 t}{1 + q_e K_2 t} \tag{7}$$

Likewise, Equation (8) represents the mathematical model of the linearization of Equation (7). The values of K_2 and *qe* can be obtained with the intercept and slope of the curve, respectively, presented in the graph (*t/qt*) according to *t* [22]:

$$\frac{t}{q_t} = \frac{1}{K_2 q_e^2} + \frac{1}{q_e} t \tag{8}$$

2.6. Quantification of metals

The metals were quantified before and after adsorption with an Inductively Coupled Plasma Optical Emission Spectrometry (ICP-OES). The best parameters of adsorption studies were compared with the CONAMA limits, showing the potential for removing the metal ions studied with BPF and MEC adsorbents in the conditions presented. Previously, the analytical curve was made with monoelemental reference standards at a concentration of 100 mg L^{-1} (SpecSol) for reading the samples. The analysis method was validated with the "Environmental Matrix Reference Material—A trace elements fortified sample" for use as a calibration standard (TMDA 62.2, lot 0618) from the Environment and Climate Change Canada Proficiency Testing Studies (A2LA-Accredited), which presented satisfactory results.

3. RESULTS

3.1. Characterization of banana peel flour

Considering the physical (grinding and drying) and chemical (acid treatment) treatments applied to BPF, the lignocellulosic structure is altered by the degradation of long chain structures such as lignin and hemicellulose, which makes the hydroxyl groups (-OH) of cellulose more available [23]. It also attributes higher porosity and larger surface area, thus improving the adsorptive capacity of bioadsorbents [23–24]. Figure 1 evidences these changes by characterizing the BPF bioadsorbent with Scanning Electron Microscopy (SEM), Energy-Dispersive X-Ray (EDX), and Fourier Transform Infrared Spectroscopy (FTIR).

Figures 1(a) and 1(b) represent the images obtained in the SEM of banana peel flour before (BPF-IN) and after the acid treatment (BPF-AC), respectively. Before the acid treatment, this bioadsorbent material has smooth surfaces with a low porous aspect. After the acid treatment, its surface morphology changed, forming a rougher surface with a more porous aspect, which is an essential attribute to increasing the adsorptive capacity of this material [25]. These results are expected because the acid solution applied to BPF ruptures structures such as lignin and holocellulose in the biomass [26] and attributes a high reactivity to fibers due to polarization [27], opening new active sites by removing potential pre-existing metals with acid desorption and promoting higher efficiency in adsorbing metal ions in aqueous solutions [23].

This desorption process is evidenced in the EDX spectra of the components in the BPF sample (Figure 1(c)). The BPF-IN sample shows elements such as carbon (C), oxygen (O), and potassium (K), while BPF-AC shows the removal of element K, confirming the efficiency of acid pretreatment in removing pre-existing metals in BPF but preserving elements C and O that composes the structure of the BPF lignocellulosic bioadsorbent. The gold element (Au) is present in both parts due to the metallization process to be analyzed in SEM.

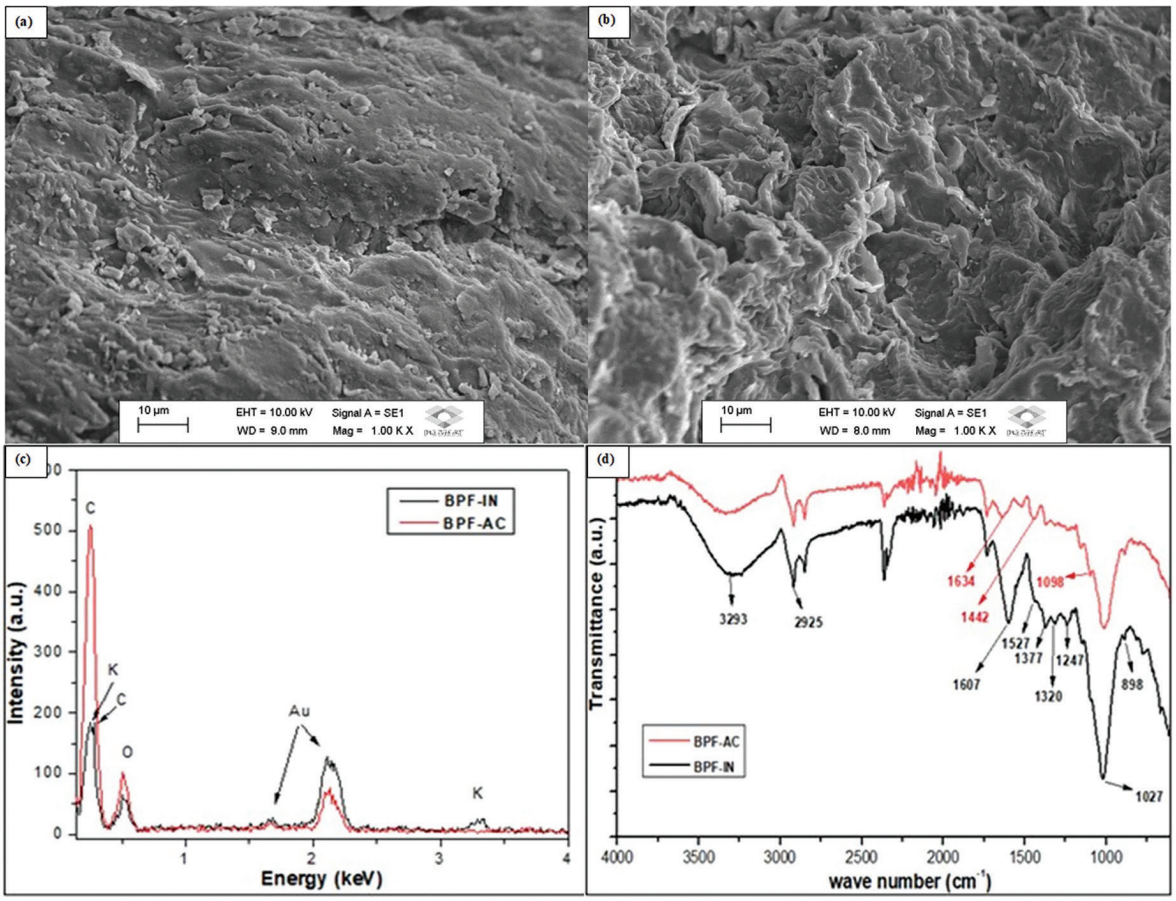

Figure 1: Characterization of banana peel flour (BPF). (a) SEM analysis before the acid treatment (BPF-IN); (b) SEM analysis after the acid treatment (BPF-AC); (c) BPF energy-dispersive X-ray analysis; (d) Spectra in the BPF infrared region.

In Figure 1(d), the FTIR spectra of BPF-IN and BPF-AC samples of the bioadsorbent indicate the presence of several organic groups potentially responsible for the adsorptive properties of this material, such as cellulose, organic acids, esters, and proteins [28]. The 3293, 2925, 1607, 1320, 1027, and 898 cm^{-1} bands of the BPF-IN sample are directly related to the organic groups of lignocellulosic materials [23]. The intense 3293 cm^{-1} band is attributed to the axial vibrational stretching of groups -OH and -NH, while the 1027 cm^{-1} band is attributed to the vibration of CO and CN groups and stretching of CH groups, which are part of the structure of lignocellulosic materials, such as cellulose, lignin, and hemicellulose [23]. The 1607, 1527, and 1320 cm^{-1} spectral bands correspond to the vibrational stretches of the C-O group of the aromatic ring that constitutes lignin. Likewise, the spectra with an intensity of 1377 and 1247 cm^{-1} correspond to the stretching of groups C-H and C-O, respectively, belonging to the acetyl functional group in hemicelluloses. As suggested in the SEM and EDX analyses, the BPF-AC sample shows an important structural change in the BPF bioadsorbent, considering that the spectral bands with the lignin and hemicellulose organic groups between 1027 and 1607 cm^{-1} were attenuated. This is justified by lignin and hemicellulose degradation through the action of the acid solution used to prepare the bioadsorbent. In contrast, the 3293 cm^{-1} and 1027 cm^{-1} bands are preserved, showing the functional groups -OH and -C-O-C, respectively, constituents of cellulose, and the small 898 cm^{-1} spectrum from the beta-glycosidic bonds among the saccharide units that compose cellulose [23]. Bioadsorption occurs through electrostatic interactions and/or the formation of bonds between metal ions and functional groups, mainly cellulose, from plant biomass [7].

3.2. Characterization of magnetic nanoparticles

Figure 2 shows the results of the characterization of magnetic nanoparticles. The magnetite nanostructure (MAG) after synthesis (Figure 2(a)) shows dispersed grains. After functionalization with chitosan (MEC), Figure 2(b) shows an agglomeration of nano-adsorbent particles that can be attributed to Van der Waals forces [16] due to the presence of functional groups such as cellulose in the polymer, which in turn, improves the adsorptive properties of the nano-adsorbent for metal ions [23].

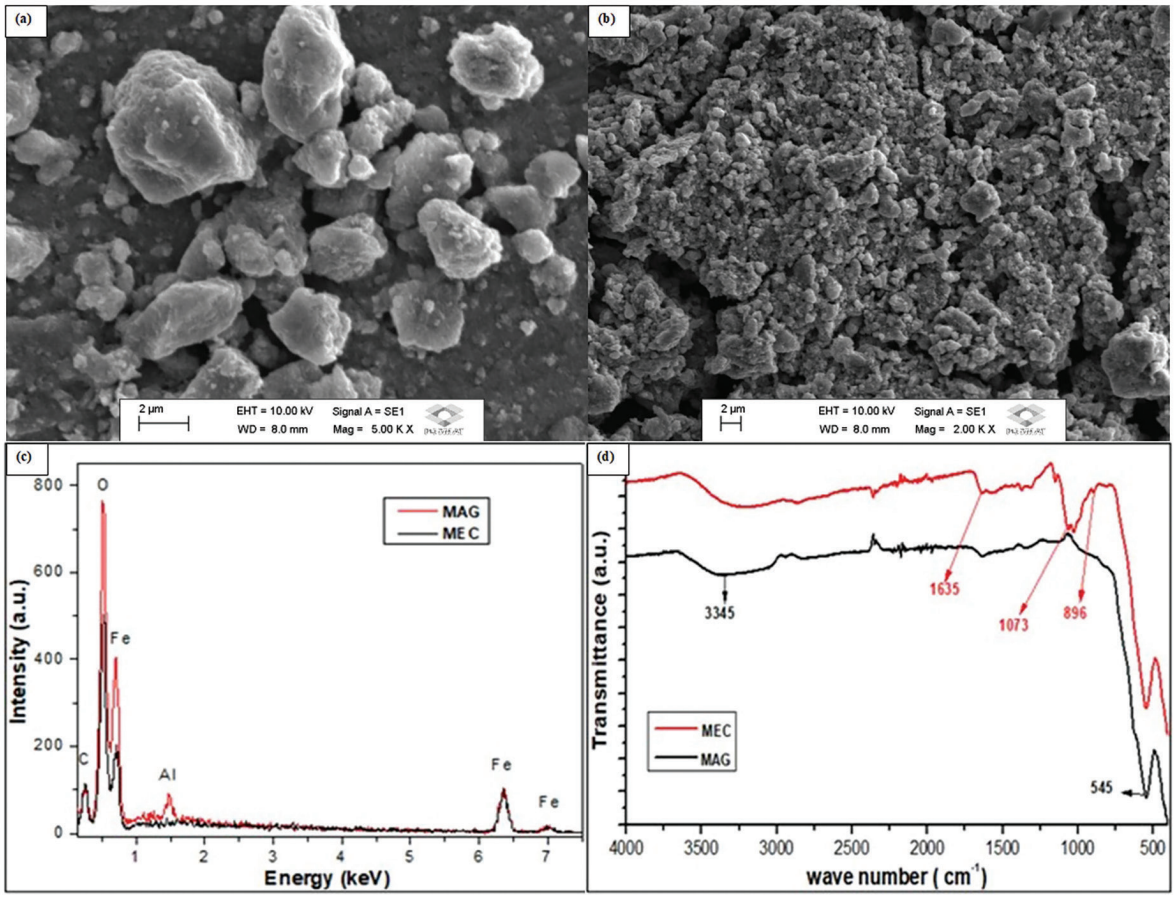

Figure 2: Characterization of the nano-adsorbent. (a) SEM analysis of magnetites (MAG); (b) SEM analysis of chitosan-encapsulated magnetite (MEC); (c) Analysis of energy-dispersive X-rays of MAG and MEC; (d) Spectra in the infrared region of MAG and MEC.

The EDX spectra of the components in the MAG and MEC samples did not show significant changes (Figure 2(c)), showing the prevalence of Fe and O, which are the basis of the molecular structure of magnetite (Fe-O and Fe-O-Fe).

The FTIR spectrum of the nano-adsorbent in Figure 2d shows, in the MAG spectrum, the 3345 cm^{-1} band that represents axial vibrational stretching of -OH groups [16], suggesting water adsorption by magnetite. The 545 cm^{-1} band in MAG and MEC can be attributed to magnetite stretching vibrations of Fe-O and Fe-O-Fe [29]. Moreover, the encapsulation of magnetite by the chitosan polymer attributed a higher adsorptive functionality to this nanomaterial, as MEC showed an increased intensity of bands intrinsic to the molecular structures in the chitosan polymer, which contributes to the removal of metal ions by having several functional groups. In this sense, the 1635 cm^{-1} band can be attributed to -NH bonds of the amino groups, the C=O bonds from the residual amide groups in the chitosan polymer, and the 1073 cm^{-1} band corresponding to the structure of the COC glucose cycle of a cellulose monomer [16]. The small 896 cm^{-1} spectrum is attributed to the beta-glycosidic bonds between the saccharide units that constitute cellulose [23]. The active sites of chitosan consist of amino and hydroxyl groups responsible for removing heavy metals from an aqueous medium [16–17]. Additionally, nanomaterials have important physical and chemical properties that contribute to adsorption, such as a large surface area and high reactivity [16].

3.3. Adsorption studies

3.3.1. Influence of pH variation on the adsorptive process

The pH value of the solution is crucial in the adsorption of metal ions, as it directly influences the interactions between the adsorbent and the adsorbate [5, 23], as observed in Figure 3.

The results show that a pH higher than 6 can achieve maximum adsorption and efficiency in the simultaneous removal of the metal ions in the PMS by BPF and MEC adsorbents. The adsorption capacity decreases

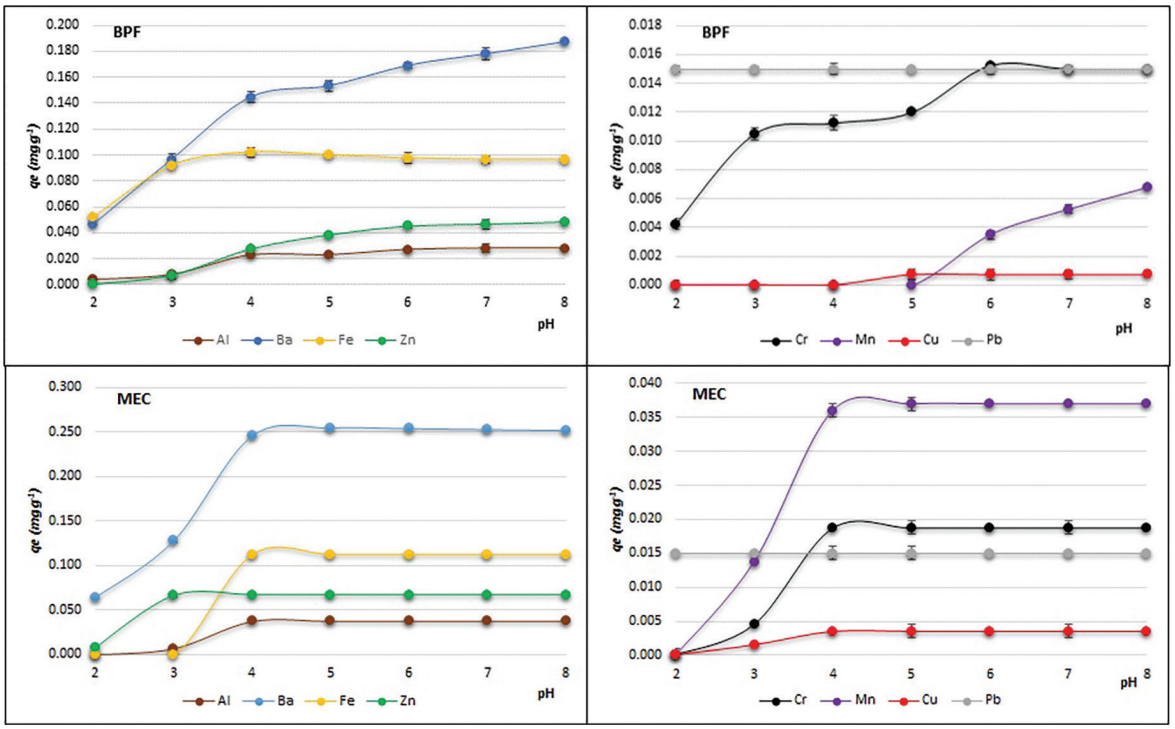

Figure 3: Quantity of metal ions adsorbed by BPF and MEC adsorbents in equilibrium (qe) according to the pH.

with the decrease in the pH value of the solution. This result suggests a competition between metal ions and protons (H^+) in the solution for the active adsorbent site, the formation of potential complexes among metals, anions, and water (solvation) with electrically neutral charges, or even the tendency of surface charges of the adsorbent to protonate due to the increase of H^+ in the solution [23]. At higher pH values, starting from a pH of 4, the system starts the adsorptive equilibrium for most metal ions in both adsorbents, except for Ba and Mn ions, which the BPF adsorbent tends to increase as the pH value increases. This phenomenon can be explained by the potential formation of hydroxy-complex species of $[(Metal).(OH)]^+$ in the solution, favoring adsorption at a higher pH than the adsorbent surface, which consists of polar groups (hydroxyls, carboxyls, amino, etc.) that are possibly negatively charged. In contrast, the formation of other complexes such as $[(Metal).(OH)_2]$ gives the system neutrality and stability, which support the balance between species and the adsorbent surface [30]. Figure 3 also shows that MEC initiates the adsorptive process of metal ions at a lower pH than BPF because, for each adsorbent, the pH value establishes the surface charge of these materials and determines the interactions between metal ions and adsorbents [30–31]. The Pb ion can be removed at a minimum pH in both adsorbents, suggesting higher compatibility between the species associated with Pb and the adsorbent surfaces in detriment to the protons (H^+) of the solution.

According to the results of this phase, the pH value was fixed at 6 for the following studies.

3.3.2. Variation in the mass of adsorbents

To determine the minimum amount of adsorbent material required for the maximum removal of metal ions simultaneously, the adsorptive study was performed with the variation in the mass of BPF and MEC adsorbents represented by the isotherms in Figure 4.

This study showed that 25 mg of both adsorbents for each 25 mL of PMS was sufficient for the maximum removal of metal ions from the fixed-concentration solution (Table 1). Thus, the data obtained corroborate the literature [5, 30] when referring to the availability and distribution of chemical species in a solution according to the pH value. Based on this assumption, the chemical species formed by the metal ions in the solution with fixed concentrations and pH value of 6 are limiting, and the increase in the amount of adsorbent material does not imply an increase in adsorption because the chemical species available are already in solid-liquid equilibrium in a minimum of 25 mg of adsorbents. Thus, there is an excess of active sites for a limited number of chemical species at a pH value of 6.

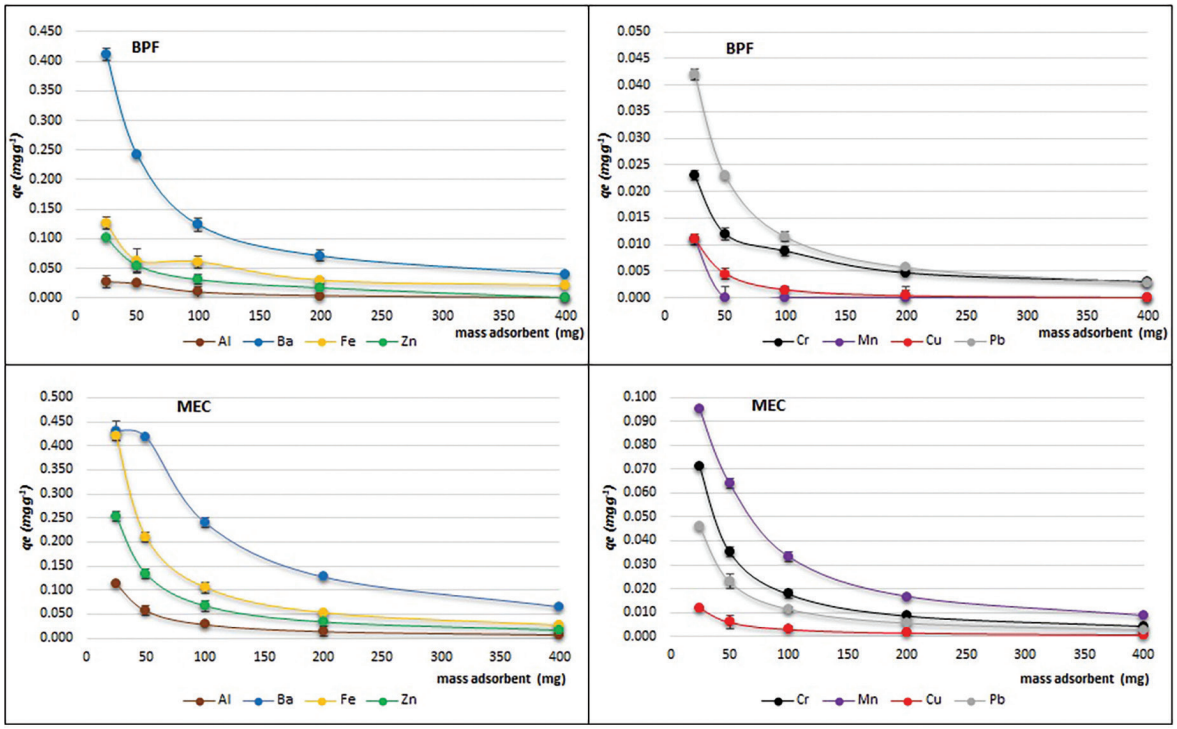

Figure 4: Amount of metal ions adsorbed by BPF and MEC adsorbents in equilibrium (qe) according to the variation in the mass of adsorbents.

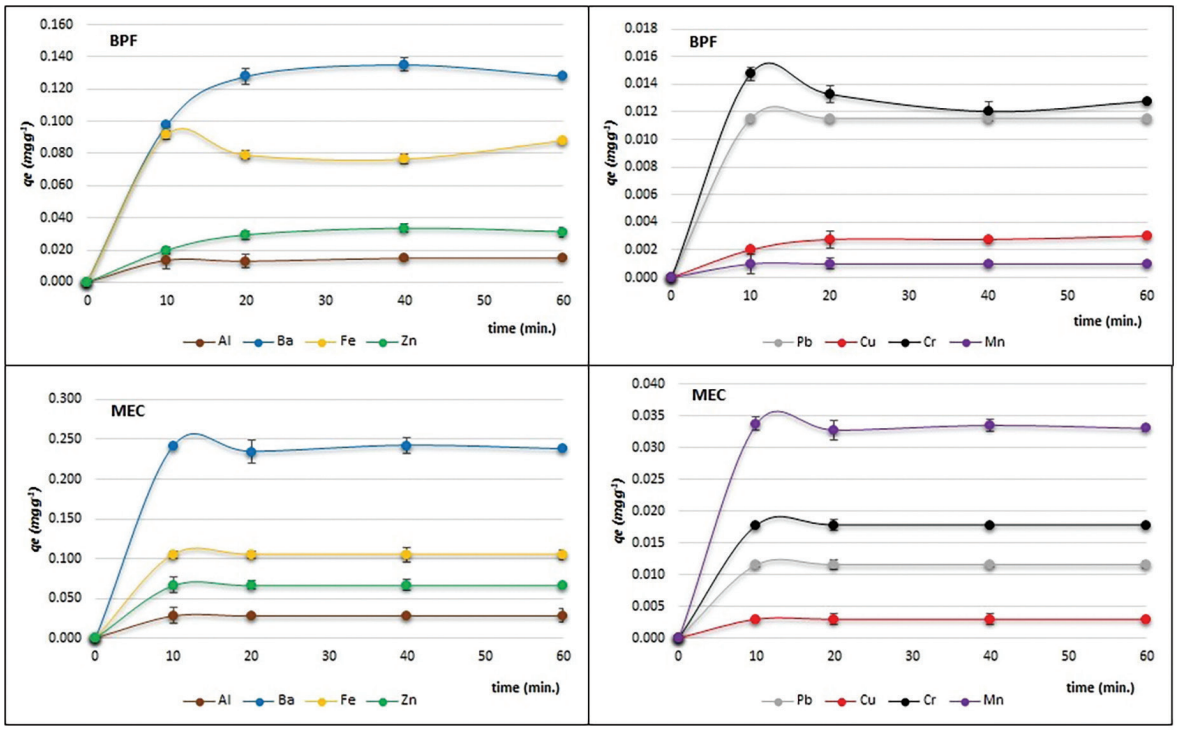

Figure 5: Amount of metal ions adsorbed by BPF and MEC adsorbents according to contact time.

3.3.3. Kinetic adsorption study

This study was performed with a pH value of 6 and 100 mg of both adsorbents. Figure 5 shows the amount of metal ions adsorbed by BPF and MEC adsorbents in equilibrium (*qe*) according to contact time. The adsorption of metal ions is relatively fast, considering that 10 minutes promoted significant adsorption. Subsequently, the

Table 2: Regression analysis of kinetic parameters of metal ion adsorption by BPF.

PSEUDO-SECOND-ORDER LINEAR					PSEUDO-SECOND-ORDER NON-LINEAR				EXPERIMENTAL
METAL IONS	R^2	K_2 (g mg^{-1} min^{-1})	qe_{cal} (mg g^{-1})	ERROR	R^2	K_2 (g mg^{-1} min^{-1})	qe_{cal} (mg g^{-1})	ERROR	qe_{exp} (mg g^{-1})
Al	0.99	61.6	0.015	9×10^{-4}	0.99	50.3	0.015	6×10^{-4}	0.014
Ba	0.99	6.51	0.133	1×10^{-3}	0.98	1.68	0.145	8×10^{-3}	0.132
Pb	0.99	178.3	0.012	6×10^{-5}	1.00	1×10^{15}	0.011	2×10^{-17}	0.012
Cu	0.99	126.8	0.003	5×10^{-5}	0.98	54.6	0.003	2×10^{-4}	0.003
Cr	0.99	254.8	0.013	1×10^{-4}	0.96	3×10^{43}	0.013	6×10^{-4}	0.013
Fe	0.98	16.8	0.085	1×10^{-3}	0.97	-3×10^{43}	0.084	3×10^{-3}	0.084
Mn	0.99	434.2	0.001	2×10^{-4}	1.00	6×10^{15}	0.001	1×10^{-17}	0.001
Zn	0.99	189.7	0.038	4×10^{-4}	0.97	3.50	0.038	3×10^{-3}	0.038

qe_{exp}: Experimental adsorptive capacity; qe_{cal}: Calculated adsorptive capacity.

Table 3: Regression analysis of kinetic parameters of metal ion adsorption by MEC.

PSEUDO-SECOND-ORDER LINEAR					PSEUDO-SECOND-ORDER NON-LINEAR				EXPERIMENTAL
METAL IONS	R^2	K_2 (g mg^{-1} min^{-1})	qe_{cal} (mg g^{-1})	ERROR	R^2	K_2 (g mg^{-1} min^{-1})	qe_{cal} (mg g^{-1})	ERROR	qe_{exp} (mg g^{-1})
Al	0.99	99.9	0.029	2×10^{-4}	1.00	144.4	0.029	3×10^{-4}	0.029
Ba	0.99	246.1	0.239	8×10^{-4}	0.99	-4×10^{43}	0.24	1×10^{5}	0.239
Pb	0.99	178.7	0.012	6×10^{-5}	1.00	1×10^{15}	0.011	2×10^{-17}	0.012
Cu	0.99	346.8	0.003	2×10^{-4}	1.00	4×10^{14}	0.003	1×10^{-18}	0.003
Cr	0.99	119.6	0.018	1×10^{-4}	1.00	3×10^{14}	0.018	8×10^{-17}	0.018
Fe	1.00	214.7	0.105	5×10^{-4}	1.00	3×10^{12}	0.105	2×10^{-14}	0.105
Mn	0.99	114.3	0.034	4×10^{-5}	0.99	-3×10^{43}	0.033	3×10^{-4}	0.034
Zn	0.99	123.4	0.067	4×10^{-4}	1.00	7×10^{13}	0.067	8×10^{-16}	0.067

qe_{exp}: Experimental adsorptive capacity; qe_{cal}: Calculated adsorptive capacity.

system remains in equilibrium, in which all active sites of the adsorbents have been potentially filled or the metal species available in the solution have been adsorbed, as previously discussed.

The contact time of 10 minutes to reach adsorptive equilibrium suggests adsorption characteristics by the physical interaction between adsorbents and adsorbates. Physisorption occurs at nonspecific active sites and the entire adsorbent surface. Theoretically, from a thermodynamic point of view, the energy involved is slightly low (less than 10 Kcal mol^{-1}; energetic order of vaporization and condensation), thus adding speed and reversibility to the adsorptive interaction of species [23, 32]. The results of the pH variation study corroborate the suggestion of physical adsorption, as alternating charges between the chemical species available in the medium and the charges of adsorbents surfaces according to the pH evidenced the electrostatic interaction between the ions and the surface.

However, the data obtained by applying kinetic models to the interactions of metal ions with BPF and MEC adsorbents revealed that the pseudo-second-order model [22] was better adjusted because the linear correlation coefficients (R^2) were near 1, corroborating the literature [16, 33]. The pseudo-first-order model, in turn, presented very low R^2 values, attributing an unfavorable adjustment. Moreover, the *qe* experimental values (Figure 5) agree with the theoretically calculated values, showing small differences (errors) between these variables and confirming that adjusting the pseudo-second-order model favors the adsorptive process studied, according to the data in Tables 2 and 3 for BPF and MEC adsorbents, respectively. The graphs used to obtain the results in Tables 2 and 3 are in the Supplementary Material.

Adsorption kinetics is influenced by the concentration of adsorbate ions and the number of sites available for interacting with metals [34], which resulted in the high values of K_2 velocity constants (g mg^{-1} min^{-1}) found experimentally in this study and that determined the rapid deposition of metal ions in the adsorbents.

4. DISCUSSION

Adsorbent treatments have been extensively and successfully used, considering that such specific processes modify the adsorbent and increase the adsorptive capacity of these materials [35]. This study explained, with SEM, EDX, and FTIR, the importance of acid pretreatment to BPF and the encapsulation of magnetite by chitosan. Considering the removal of inorganic elements and organic structures, pretreatment is essential to enhance the adsorptive capacity of the BPF lignocellulosic bioadsorbent [5, 23]. In MEC, it added essential organic groups for metal removal. Another important chitosan property is the improvement in the colloidal stability of the magnetic nanoparticle, a crucial attribute for removing ionized metals in aqueous solutions [17]. Therefore, the literature cites the importance of using bioadsorbents or biopolymers to remove metal ions simultaneously in an aqueous medium with satisfactory results, and Fe (II), Zn (II), Mn (II), Cu (II), Pb (II), Co (III), Ni (II), Cr (III), and V (IV) stand out among these metal ions [34, 36, 37]. It is worth noting that BPF and chitosan are the bioadsorbents used in this study.

The adsorptive capacity of BPF and MEC adsorbents evidenced in adsorption studies using the isotherms of variations in pH values and mass of the adsorbents and contact time corroborate the results presented by the SEM, EDX, and FTIR of adsorbents after adsorption, illustrated in Figure 6. Therefore, the SEM results of the BPF adsorbent after adsorption (BPF-AD) (Figure 6(a)) suggest the filling of surfaces that were previously rougher (Figure 1(b)) by the potential adsorption of metal ions. This statement corroborates the data obtained in the composition analysis with EDX (Figure 6(b)) that indicated the presence of Al and Pb ions after adsorption, which may imply that this bioadsorbent is effective in removing metal ions in aqueous solutions. The SEM results of MEC after adsorption (MEC-AD) (Figure 6(d)) did not show significant visual changes after the adsorptive process. However, the composition analysis with EDX (Figure 6(e)) showed the presence of Zn (II) and Al (III) metals on the nano-adsorbent surface, indicating the potential of this material. The other metals in the solution were not observed, possibly due to the limitation and low sensitivity of the equipment in the analysis of metal traces [38]. The FTIR data of the BPF-AD sample, compared to the BPF-AC sample, (Figure 6(c)), showed attenuation in the intensity of the 1098 cm^{-1} band, an increase in the intensity of the 1239 cm^{-1} band, and a small displacement in the 1442 cm^{-1} and 1634 cm^{-1} spectra, suggesting the incorporation of metal ions by adsorption and consequently the formation of the metal-adsorbent complex with the functional groups available in BPF [23]. Likewise, FTIR data from the MEC-AD sample, compared to MEC (Figure 6(f)), showed a significant attenuation of the intensities of 1073 and 1635 cm^{-1} spectra, suggesting the adsorption of metal ions and formation of the metal/adsorbent complex with the functional groups available in chitosan. The 545 cm^{-1} spectrum intrinsic to magnetite was attenuated and still experienced a small displacement of 13 cm^{-1}, which shows that the Fe-O and Fe-O-Fe magnetite bonds were distorted after metal ion adsorption.

Finally, gathering the best parameters of adsorption studies for each adsorbent allowed evaluating the potential and percentage of removal of each metal ion in the PMS with concentrations higher than those allowed in the Brazilian legislation.

Figure 7 presents the results of experiments to remove metal ions with BPF and MEC adsorbents in PMS. The removal of Al (III), Ba (II), Pb (II), Cu (II), Cr (III), Fe (II), Mn (II), and Zn (II) ions by MEC showed higher efficiency than BPF, being higher in the following percentages: 53.6, 31.9, 3.4, 50.0, 37.2, 33.5, 82.7, and 53.1%, respectively. However, the BPF bioadsorbent was efficient and promising because removal percentages between 43.9 and 96.6% suggest that the modified banana peel can remove metal ions from effluent samples. As an exception, the removal of the Mn metal did not reach high percentages in the conditions studied – only 5.3% –, which may be attributed to the affinity factors between Mn ions and the adsorption sites of the bioadsorbent. This indicates that the pH of 6 and the presence of other metal ions in the medium (Figure 3) determined the decrease in adsorptive capacity of BPF for the Mn ion. Other studies indicate that a bioadsorbent removing the Mn ion is favorable, with percentages higher than 60% for the same pH value but in monoelemental conditions [33, 39]. However, a higher affinity of Mn and Cr ions for MEC could be measured even in the presence of other metal ions, suggesting the formation of species in the

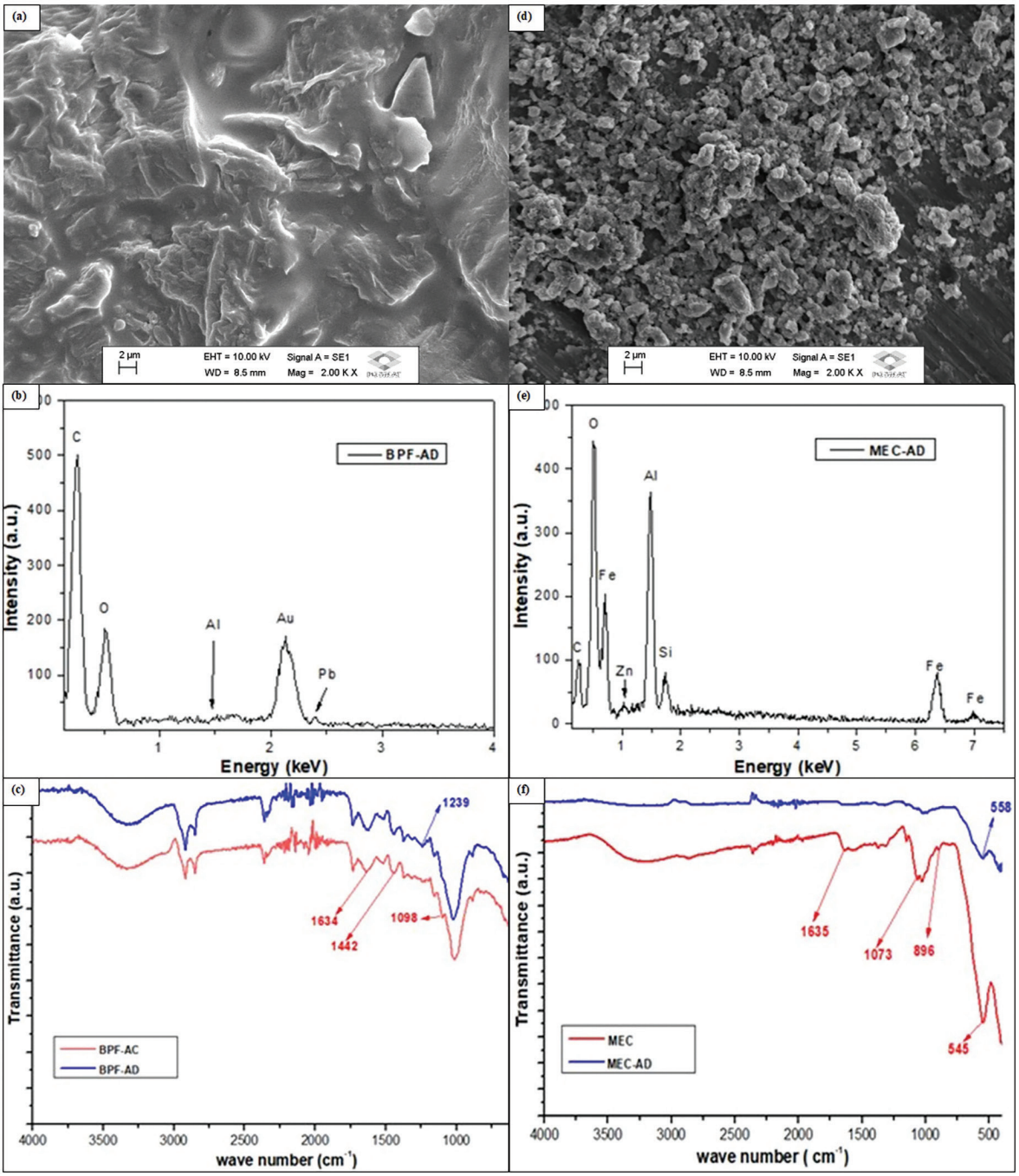

Figure 6: Characterization of BPF and MEC adsorbents after adsorption. (a) SEM analysis of BPF after adsorption (BPF-AD); (b) EDX from BPF-AD; (c) Spectra in the infrared region of BPF-AC and BPF-AD; (d) SEM analysis of MEC-AD; (e) EDX from MEC-AD; (f) Spectra in the infrared region of MEC and MEC-AD.

solution that are more compatible with magnetite (Fe_3O_4) and/or the abundant amino groups in chitosan in the modified nano-adsorbent [40–43].

It is worth mentioning that both adsorbents were promising in complying with the Brazilian legislation recommended by the CONAMA, considering that the removal of metal ions by both adsorbents in aqueous solutions above the limits, in the conditions studied, was satisfactory, except for the removal of Mn by BPF.

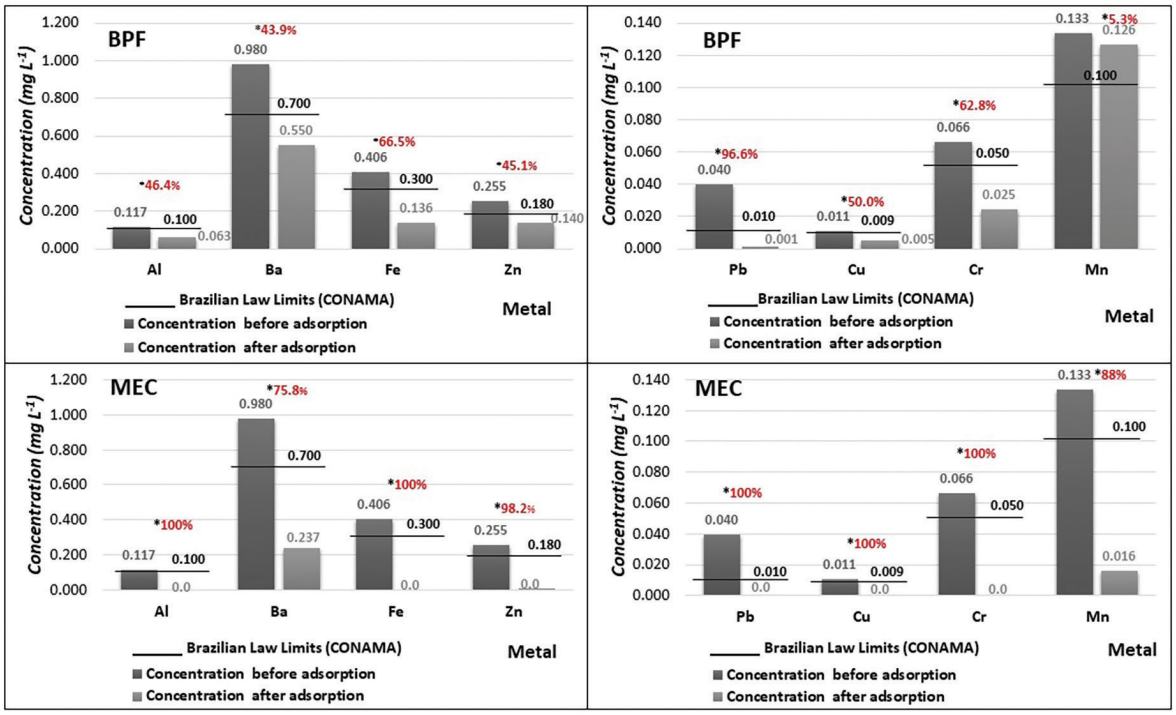

Figure 7: Adsorption results using the best parameters of heavy metal ion remediation studies in the prepared metal solution. *Represents the percentage of removal of each metal after adsorption.

5. CONCLUSIONS

The results obtained in this study allow concluding that BPF and MEC adsorbents are promising for remediating heavy metal ions in an aqueous medium. The application of pretreatment methods to BPF and the encapsulation of magnetite by chitosan were adequate and essential for metal ion adsorption. The characterizations by SEM, EDX, and FTIR allowed understanding the improvements in the adsorptive capacity of both adsorbents. The FTIR method confirmed the existence of functional groups in both adsorbents that are responsible for the adsorptive interaction with metal ions in aqueous solutions, such as hydroxyls and amino groups. Adsorption studies helped determine the best adsorptive parameters for the bioadsorbent and nano-adsorbent. The most adequate pH range was between 6 and 8, the mass of adsorbents with the best efficiency was 25 mg, and the contact time was 10 minutes, which may suggest that the interaction between adsorbents and metal ions occurs by physical adsorption, as the process was fast. The parameters obtained with the application of the kinetic models to both adsorbents showed that the pseudo-second-order model was better adjusted. Concomitantly, the SEM, EDX, and FTIR analyses confirmed the adsorptive capacity of both adsorbents in metal ion solutions. Subsequently, gathering the best parameters of the adsorption study allowed concluding that both adsorbents are highly capable of removing metal ions in aqueous solutions and contribute as alternative materials to comply with the Brazilian legislation regarding the reduction of heavy metal ions in effluents. However, MEC was more efficient than BPF in the simultaneous removal of metal ions in PMS. Thus, the removal of metal ions by MEC can be classified in the order of higher efficiency: Al=Fe=Pb=Cu=Cr>Zn>Mn>Ba, in the percentages of 100, 100, 100, 100, 100, 98, 88, and 76%, respectively. BPF was removed in the following order: Pb>Fe>Cr>Cu>Al>Zn>Ba>Mn, in the percentages of 97, 67, 63, 50, 46, 45, 44, and 5%, respectively. The affinity between adsorbents with some metal ions is due to the characteristics of the adsorbent surface and the number of chemical species available in the solution according to the pH value of the medium.

Finally, due to the interest in acquiring alternative and economically viable materials with the potential for treating effluents containing various heavy metal ions, the BPF and MEC adsorbents were effective due to their high ability to simultaneously remove several ionized metal pollutants in proper conditions.

6. BIBLIOGRAPHY

[1] LEANDRO-SILVA, E., PIPI, A.R.F., MAGDALENA, A.G., *et al.,* "Aplicação dos modelos de Langmuir e Freundlich no estudo da casca de banana como bioadsorvente de cobre (II) em meio aquoso", *Matéria (Rio J.)*, v. 25, n. 2, e-12656, 2020. https://doi.org/10.1590/S1517-707620200002.1056

[2] HOSSAIN, M.A., NGO, H.H., GUO, W.S., *et al*., "Removal of copper from water by adsorption onto banana peel as bioadsorbent", *International Journal of GEOMATE*, v. 2, n. 2, pp. 227–234, 2012.

[3] ANNADURAI, G., JUANG, R.S., LEE, D.J., "Adsorption of heavy metals from water using banana and orange peels", *Water Science & Technology,* v. 47, n. 1, pp. 185–190, 2003. https://doi.org/10.2166/wst.2003.0049

[4] VAGHETTI, J.C.P., *Utilização de biossorventes para remediação de efluentes aquosos contaminados com metais metálicos.* Tese (Doutorado em Química), Universidade Federal do Rio Grande do Sul, Porto Alegre, 2009.

[5] CRUZ, M.A.R.F., *Utilização da casca de banana como biossorvente.* Dissertação (Mestrado em Química dos Recursos Naturais), Universidade Estadual de Londrina, Londrina, 2009.

[6] SOUSA, F.W., MOREIRA, S.A., OLIVEIRA, A.G., *et al.,* "The use of green coconut shells as absorbents in the toxic metals", *Química Nova,* v. 30, n. 5, pp. 1153–1157, 2007. https://doi.org/10.1590/S0100-40422007000500019

[7] RODRIGUES, R.F., TREVENZOLI, R.L., SANTOS, L.R.G., *et al.,* "Heavy metals sorption on treated wood sawdust", *Engenharia Sanitaria e Ambiental,* v. 11, n. 1, pp. 21–26, 2006. https://doi.org/10.1590/S1413-41522006000100004

[8] BARROS, A.M., *Bioadsorção e dessorção dos íons Cd2+, Cu2+, Ni2+, Pb2+ e Zn2+ pela macrófita aquática azolla pinnata.* Dissertação (Mestrado em Engenharia Química), Universidade Estadual de Campinas, Campinas, 2012.

[9] CARVALHO, L.R., AGUIAR-OLIVEIRA, E., KAMIMURA, *et al.,* "Bioadsorção de crômio (VI) em casca de banana nanica (Musa paradisíaca L.) em pó em frascos agitados e em leito fixo", In: *XVI Congresso Brasileiro de Engenharia Química–EMBEC*, Fortaleza, 2016.

[10] MARTINS, W.A., DE OLIVEIRA, A.M.B.M., DE MORAIS, C.E.P., *et al.,* "Reaproveitamento de resíduos agroindustriais de casca banana para tratamento de efluentes", *Revista Verde de Agroecologia e Desenvolvimento Sustentável,* v. 10, n. 1, pp. 96–102, 2015. https://doi.org/10.18378/rvads.v10i1.3361

[11] ROCHA, C.G., ZAIA, D.A.M., ALFAYA, R.V.S., *et al.,* "Use of rice straw as biosorbent for removal of Cu(II), Zn(II), Cd(II) and Hg(II) ions in industrial effluents", *Journal of Hazardous Materials,* v. 166, n. 1, pp. 383–388, 2009. https://doi.org/10.1016/j.jhazmat.2008.11.074

[12] OH, J.K., Park, J.M., "Iron oxide-based superparamagnetic polymeric nanomaterials: Design, preparation, and biomedical application", *Progress in Polymer Science,* v. 36, n. 1, pp. 168–189, 2011. https://doi.org/10.1016/j.progpolymsci.2010.08.005

[13] YAMAURA, M., CAMILO, R.L., SAMPAIO, L.C., *et al.,* "Preparation and characterization of (3-aminopropyl) triethoxysilane-coated magnetite nanoparticles", *Journal of Magnetism and Magnetic Materials,* v. 279, n. 2–3, pp. 210–217, 2004. https://doi.org/10.1016/j.jmmm.2004.01.094

[14] ZHANG, X., ZHANG, P., WU, Z., *et al.,* "Adsorption of methylene blue onto humic acid-coated Fe_3O_4 nanoparticles", *Colloids and Surfaces A: Physicochemical and Engineering Aspects,* v. 435, pp. 85–90, 2013. https://doi.org/10.1016/j.colsurfa.2012.12.056

[15] ZHOU, C., WU, Z., ZHANG, W., *et al.,* "Facile synthesis of humic acid-coated iron oxide nanoparticles and their applications in wastewater treatment", *Functional Materials Letters,* v. 4, n. 4, pp. 373–376, 2011. https://doi.org/10.1142/S1793604711002238

[16] MATEI, E., PREDESCU, A.M., RÂPĂ, M., *et al.,* "Removal of Chromium(VI) from aqueous solution using a novel green magnetic nanoparticle – chitosan adsorbent", *Analytical Letters,* v. 52, n. 15, pp. 2416–2438, 2019. https://doi.org/10.1080/00032719.2019.1601734

[17] BOLISETTY, S., PEYDAYESH, M., MEZZENGA, R., *et al.,* "Sustainable technologies for water purification from heavy metals: review and analysis", *Chemical Society Reviews*, v. 48, n. 2, pp. 463–487, 2019. https://doi.org/10.1039/C8CS00493E

[18] MAGDALENA, A.G., SILVA, I.M.B., MARQUES, R.F.C., *et al.,* "EDTA-functionalized Fe_3O_4 nanoparticles", *Journal of Physics and Chemistry of Solids,* v. 113, pp. 5–10, 2018. https://doi.org/10.1016/j.jpcs.2017.10.002

[19] CONSELHO NACIONAL DO MEIO AMBIENTE (CONAMA). Dispõe sobre as condições e padrões de lançamento de efluentes, complementa e altera a resolução n° 357, de 17 de março de 2005. Brasília: Diário Oficial, 2005.

[20] CONSELHO NACIONAL DO MEIO AMBIENTE (CONAMA). Resolução n°430, de 13 de maio de 2011. Dispõe sobre as condições e padrões de lançamento de efluentes, complementa e altera a resolução n° 357, de 17 de março de 2005. Brasília: Diário Oficial, 2011.

[21] LAGERGREN, S., "About the theory of so-called adsorption of soluble substances", *Sven. Vetenskapsakad. Handingarl*, v. 24, pp. 1–39, 1898.

[22] HO, Y.S., MCKAY, G.*,* "A kinetic study of dye sorption by biosorbent waste product pith", *Resources, conservation and recycling*, v. 25, n. 3–4, pp. 171–193, 1999.

[23] NASCIMENTO, R.F.D., SOUSA NETO, V.D.O., MELO, D.D.Q., *Uso de bioadsorventes lignocelulósicos na remoção de poluentes de efluentes aquosos*. Fortaleza: Imprensa Universitária, 2014.

[24] CANILHA, L., SANTOS, V.T.O., ROCHA, G.J.M., *et al.,* "A study on the pretreatment of a sugarcane bagasse sample with dilute sulfuric acid", *Journal of Industrial Microbiology and Biotechnology,* v. 38, n. 9, pp. 1467–1475, 2011. https://doi.org/10.1007/s10295-010-0931-2

[25] Thirumavalavan, M., LAI, Y.L., LEE, J.F., "Fourier transform infrared spectroscopic analysis of fruit peels before and after the adsorption of heavy metal ions from aqueous solution", *Journal of Chemical & Engineering Data,* v. 56, n. 5, pp. 2249–2255, 2011. https://doi.org/10.1021/je101262w

[26] CHEN, W.H., XU, Y.Y., HWANG, W.S., *et al.,* "Pretreatment of rice straw using an extrusion/extraction process at bench-scale for producing cellulosic ethanol", *Bioresource Technology,* v. 102, n. 22, pp. 10451–10458, 2011. https://doi.org/10.1016/j.biortech.2011.08.118

[27] MARTÍN, C., ALMAZÁN, O., MARCET, M., *et al.,* "A study of three strategies for improving the fermentability of sugarcane bagasse hydrolysates for fuel ethanol production", *International Sugar Journal*, v. 109, n. 1297, pp. 33–39, 2007.

[28] MEMON, J.R., MEMON, S.Q., BHANGER, M.I., *et al.,* "Characterization of banana peel by scanning electron microscopy and FT-IR spectroscopy and its use for cadmium removal", *Colloids and Surfaces B: Biointerfaces,* v. 66, n. 2, pp. 260–265, 2008. https://doi.org/10.1016/j.colsurfb.2008.07.001

[29] YAMAURA, M., FUNGARO, D.A.*,* "Synthesis and characterization of magnetic adsorbent prepared by magnetite nanoparticles and zeolite from coal fly ash", *Journal of Materials Science,* v. 48, n. 14, pp. 5093–5101, 2013. https://doi.org/10.1007/s10853-013-7297-6

[30] NASCIMENTO, R.F., LIMA, A.C.A., VIDAL, C.B., *et al., Adsorção: aspectos teóricos e aplicações ambientais*. Fortaleza: Imprensa Universitária, 2014.

[31] BAUTISTA-TOLEDO, I., FERRO-GARCÍA, M.A., RIVERA-UTRILLA, J., *et al.,* "Bisphenol a removal from water by activated carbon. effects of carbon characteristics and solution chemistry", *Environmental science & technology,* v. 39, n. 16, pp. 6246–6250, 2005. https://doi.org/10.1021/es0481169

[32] Ruthven, D.M., *Principles of adsorption and adsorption processes*. Hoboken: Wiley-Interscience, 1984.

[33] MAHLANGU, J.M., SIMATE, G.S., DE BEER, M., *et al.,* "Adsorption of Mn^{2+} from the acid mine drainage using banana peel", *International Journal of Water and Wastewater Treatment,* v. 4, n. 1, pp. 153–159, 2018. https://doi.org/10.16966/2381-5299.153

[34] ANUSH, S.M., VISHALAKSHI, B., "Modified chitosan gel incorporated with magnetic nanoparticle for removal of Cu(II) and Cr(VI) from aqueous solution", *International Journal of Biological Macromolecules,* v. 133, pp. 1051–1062, 2019. https://doi.org/10.1016/j.ijbiomac.2019.04.179

[35] MELO, D.Q., SOUSA NETO, V.O., BARROS, F.C.F., *et al.,* "Chemical modifications of lignocellulosic materials and their application for removal of cations and anions from aqueous solutions", *Journal of Applied Polymer Science,* v. 133, n. 15, pp. 1–22, 2016. https://doi.org/10.1002/app.43286

[36] DONNER, M.W., ARSHAD, M., ULLAH, A., *et al.,* "Unravelled keratin-derived biopolymers as novel biosorbents for the simultaneous removal of multiple trace metals from industrial wastewater", *Science of The Total Environment,* v. 647, pp. 1539–1546, 2019. https://doi.org/10.1016/j.scitotenv.2018.08.085

[37] MIRETZKY, P., SARALEGUI, A., CIRELLI, A.F., *et al.,* "Aquatic macrophytes potential for the simultaneous removal of heavy metals (Buenos Aires, Argentina)", *Chemosphere,* v. 57, n. 8, pp. 997–1005, 2004. https://doi.org/10.1016/j.chemosphere.2004.07.024

[38] LABORATÓRIO DE RECURSOS ANALÍTICOS E DE CALIBRAÇÃO (LRAC). *Documento orientativo,* 2017. https://www.feq.unicamp.br/index.php/lrac2

[39] ALI, A., SAEED, K., "Decontamination of Cr(VI) and Mn(II) from aqueous media by untreated and chemically treated banana peel: a comparative study", *Desalination and Water Treatment,* v. 53, n. 13, pp. 3586–3591, 2015. https://doi.org/10.1080/19443994.2013.876669

[40] HUANG, G., ZHANG, H., SHI, J.X., *et al.,* "Adsorption of chromium(VI) from aqueous solutions using cross-linked magnetic chitosan beads", *Industrial & Engineering Chemistry Research,* v. 48, n. 5, pp. 2646–2651, 2009. https://doi.org/10.1021/ie800814h

[41] KUMAR, M.N.V.R., "A review of chitin and chitosan applications", *Reactive and Functional Polymers,* v. 46, n. 1, pp. 1–27, 2000. https://doi.org/10.1016/S1381-5148(00)00038-9

[42] THINH, N.N., HANH, P.T.B., HA, L.T.T., *et al.,* "Magnetic chitosan nanoparticles for removal of Cr(VI) from aqueous solution", *Materials Science and Engineering: C,* v. 33, n. 3, pp. 1214–1218, 2013. https://doi.org/10.1016/j.msec.2012.12.013

[43] WU, F.C., TSENG, R.L., JUANG, R.S., *et al.,* "Kinetic modeling of liquid-phase adsorption of reactive dyes and metal ions on chitosan", *Water Research,* v. 35, n. 3, pp. 613–618, 2001. https://doi.org/10.1016/S0043-1354(00)00307-9

SUPPLEMENTARY MATERIAL

The following online material is available for this article:

SM1 – Graphs used to obtain the results presented in Table 2 – Kinetic parameters of the adsorption of metal ions by BPF.

SM2 – Graphs used to obtain the results presented in Table 3 – Kinetic parameters of the adsorption of metal ions by MEC.